320 *Macromolecules* **2011**, *44*, 320–324
DOI: 10.1021/ma102348g

Macromolecules
ARTICLE

Hybrid Solvents Incubated $\pi-\pi$ Stacking in Quenched Conjugated Polymer Resolved by Multiscale Computation

Cheng K. Lee,[†] Chi C. Hua,*[,†] and Show A. Chen[‡]

[†]*Department of Chemical Engineering, National Chung Cheng University, Chia-Yi 621, Taiwan, R.O.C., and* [‡]*Department of Chemical Engineering, National Tsing Hua University, Hsin-Chu 30013, Taiwan, R.O.C.*

Received October 14, 2010; Revised Manuscript Received December 9, 2010

ABSTRACT: Multiscale computations were utilized to resolve the detailed solvent−polymer interactions in binary (aliphatic/aromatic) solvent media of a standard amphiphilic conjugated polymer, poly(2-methoxy-5-(2′-ethylhexyloxy)-1,4-phenylenevinylene) (MEH-PPV), revealing an unequivocal pathway specific solvents or hybrid solvents impact the nanomorphology in the eventual quenching state. The significant finding is that, through sophisticatedly compromised, local-phase solvent particle distribution encompassing the polymer chain, certain solvent compositions (i.e., chloroform/chlorobenzene = 2:1 and chloroform/toluene = 1:1 in number density) were noted to bolster exceptional, highly extended chain conformations in solution, which in turn greatly facilitate the incubation of ordered $\pi-\pi$ stacking upon solvent evacuation via a relatively regular chain folding along the pivotal tetrahedral defects. Overall, the simulation helps clarify a long-standing ambiguity as to the molecular effects of specific solvents and, in particular, unveils previously unnoticed physics underlying the promising features of hybrid solvents in casting polymer thin films, as evidenced by recent experiments.

Introduction

Conducting conjugated polymers have nowadays become a popular molecular material for fabricating solution-processable polymer light-emitting diodes (PLED)[1−3] and plastic solar cells.[4−6] Among the most appealing features of exploiting long-chain organic semiconductors is the possibility of fine-tuning the optoelectronic behavior of solution-cast films by selecting different solvents or hybrid solvents.[7,8] Intrinsic stiffness arising from the conjugated chain backbone, however, has rendered the polymer generally poor solubility in usual organic solvents, and hence most practically used conducting conjugated polymers involve grafting various types and amounts of flexible alkyl/alkoxy side chains to the rigid phenyl backbone. The resulting amphiphilicity with respect to various types of solvent species, in turn, gives rise to a vast swath of possible chain conformations and aggregation morphologies, first in solution and later in the quenching film. To date, the actual (microscopic and localized) polymer−solvent interactions regulating elementary chain conformations from solution to the quenching state remain elusive and are difficult to be assessed by experimental methods.

Considering a standard case with poly(2-methoxy-5-(2′-ethylhexyloxy)-1,4-phenylenevinylene) (MEH-PPV; see a sketch in Figure 1) in a novel multiscale simulation, we address in this paper two fundamental issues imperative to the upcoming applications of conducting conjugated polymers: (1) In which ways may solvent-induced chain conformations directly impact the quenching morphologies, especially in view of the formation of ordered $\pi-\pi$ stacking that is generally deemed favorable for film or device performance improvement? (2) In this context, and considering the amphiphilicity of the polymer, can the use of hybrid solvents be advantageous at all? Answers to these still debating, sometimes controversial, issues should provide in-depth insights into the highly demanded, fine morphological controls in thin films made of prevalent polymer semiconductors.

*Corresponding author. E-mail: chmcch@ccu.edu.tw.

For the two binary (aliphatic/aromatic) solvent media investigated, i.e., chloroform/chlorobenzene (CF/CB) and chloroform/toluene (CF/T), the simulation has contributed to the first revelation of anomalous solvent particle distributions within a local-phase regime of MEH-PPV, which we demonstrate to have significant impact not only on the accessible chain conformations in solution but also for the incubation of ordered $\pi-\pi$ stacking in the quenching state. Thus, the simulation helps clarify a long-standing ambiguity as to the molecular effects of specific solvents and, in particular, unveils previously unnoticed physics underlying the promising features of hybrid solvents in casting polymer thin films, as evidenced by recent experiments.[9,10] The prime results and implications are summarized in the following sections, after a brief introduction is provided to a multiscale scheme capable of capturing single MEH-PPV chains from solution to the quenching state.

Simulation Protocols

The basic ideas underlying this multiscale computation originate from a recent progress in circumventing several inherent difficulties in capturing single-chain conformations from solution to the quenching state for high-molecular-weight polymers as typically studied in experiments.[11] And the present simulation of MEH-PPV represents the first attempt to substantiate the ideas into practically interested material properties of a standard conjugated polymer. The simulation begins with the construction of a new coarse-grained (CG) polymer model for MEH-PPV that is much more efficient for investigating the solution-state chain conformations than the counterpart full-atom model. Figure 1 depicts how a (all-trans) MEH-PPV chain may be coarse-grained by introducing suitable "superatoms" to represent essential molecular units—in this case, the repeating phenyl backbone unit and two asymmetric alkoxy side-chain groups. Likewise, solvent molecules are cast into single CG "beads" of similar size. All CG particles are mapped at the mass centers and converse the full masses of the molecular units they represent. The next step is typical of prevailing CG simulations of long-chain molecules,[11−35]

 Published on Web 12/23/2010

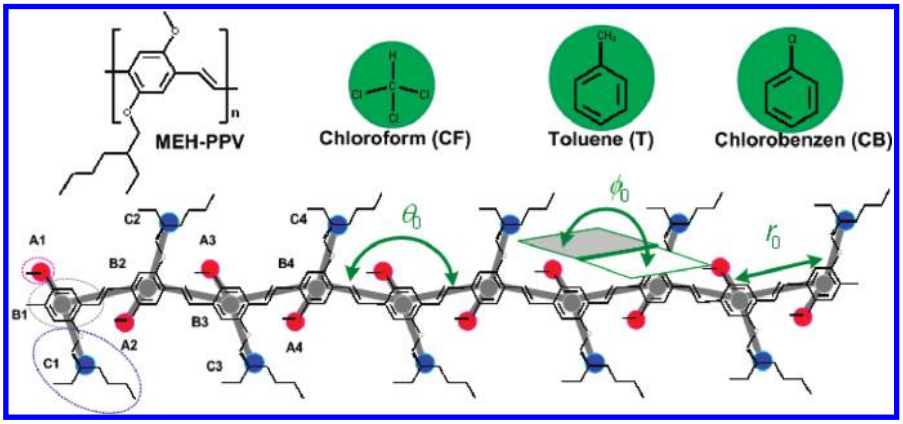

Figure 1. Specifications of a few representative bond length and angles for the CG model of MEH-PPV, where B, A, and C denote the aromatic backbone, short alkoxy, and long alkoxy side chains, respectively.

and the details can be found in previous work[11,31,35] as well as in the Supporting Information. Basically, the procedure involves the construction of self-consistent, parameter-free, intra- (bonded) or intermolecular (nonbonded) potentials governing the CG particles by using the Boltzmann inversions of essential statistical trajectories gathered from atomistic molecular dynamics (AMD) simulations of the original, atomistic models for the polymer and solvents, respectively. Additional iterative and optimization procedures are usually required in establishing the CG intermolecular potentials to account for the effect of many-body interactions. Afterward, the predicted bond-length and bond-angle (see definitions in Figure 1) distributions for a MEH-PPV oligomer from AMD and CG simulations (the latter utilizing the CG force fields already established), respectively, are checked for self-consistency and so are the predicted radial distribution functions (RDFs) for individual CG particle baths or their mixtures.

Note that the proposed CG polymer model differs from a recent one[31] in that the two side-chain groups are treated as independent CG particles rather than being lumped into the backbone unit, so as to discriminate the chemical affinities of different types of solvent molecules with respect to various parts of the polymer chain. Moreover, tetrahedral defects—a localized breakage of single/double-bond conjugation—are incorporated and assigned uniformly to every 10 repeating units on the polymer backbone in order to realistically capture the collapsed morphologies of real synthesized chains during the quenching process,[36,37] which is simulated separately by a back-mapping scheme described later. Early experiments appear to suggest that the degree of tetrahedral defects could, in general, fall below 10%,[38] yet the actual amount of defects is difficult to estimate precisely. The following results were obtained for a 300-mers MEH-PPV, close to the chain lengths of a commercial sample commonly utilized in experiment. To ensure the capability of the proposed CG system for capturing essential polymer−solvent interactions, a 10-mers MEH-PPV suspended in a binary solvent medium, i.e. CF/CB = 2:1 in number density, was first investigated in a benchmark simulation for both atomistic and CG model systems, and the predicted solvent−polymer pair distributions (see a later discussion) indicated a good agreement between the two. Both AMD and CG simulations (see Supporting Information for details) utilized the *NPT* ensemble at $T = 298$ K and $P = 1$ atm, with the same software package as described in a previous work, where the incorporated force fields were noted to lead to generally good agreement with known experimental features of MEH-PPV in solution.[31]

Results and Discussion

Solution-State Chain Conformations. Within the CG model systems described above, coarse-grained molecular dynamics (CGMD) simulations were carried out following the Newton's equations of motion for all CG particles. The results shown in Figures 2−4 were based on time (over a period of 2.5 ns) plus ensemble (for 10 independent chains) averaging for a CG model system that has been pre-equilibrated with standard Monte Carlo schemes. First, the mean radii of gyration of single MEH-PPV chain in various single- or binary-solvent media are shown in Figure 2. Note that the mean coil size often serves as a direct measure of the so-called solvent quality for the polymer in a specific solvent. Thus, the results given in Figure 2 reveal a significant feature that binary solvents of certain compositions (i.e., CF/CB = 2:1 or CF/T = 1:1) may lead to an effective solvent quality notably exceeding the ones for the two individual single solvents. The anomaly is most prominent for the case with CF/CB = 2:1, where highly extended chain conformations can frequently be noted, as partly shown by the snapshots given in Figure 4. In contrast, much collapsed chain conformations were typically noted at other mixing ratios.

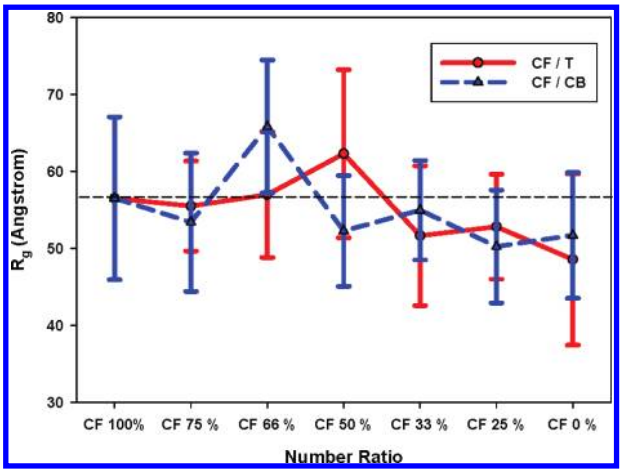

Figure 2. Predicted mean radius of gyration for single 300-mer MEH-PPV chains in single- or binary-solvent system at 298 K and 1 atm. The lines are utilized to guide the overall trend.

Given that CF arguably represents the best solvent known so far for MEH-PPV, the even surpassing solvent qualities noted in Figure 2 for two specific binary solvent media seem to be exceptional and have motivated a scrutiny into the underlying polymer−solvent interactions. An interesting general implication of the above observations with MEH-PPV is that the effective solvent quality of amphiphilic polymer solution may, to some extent, be further improved

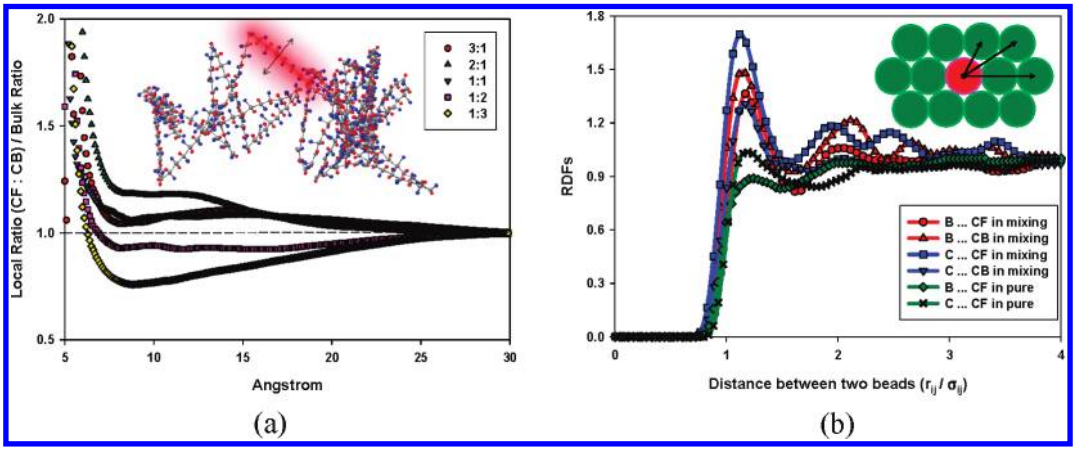

Figure 3. (a) Solvent particle distributions measured as a normal distance away from the polymer backbone in the CF/CB binary-solvent medium of MEH-PPV. (b) The RDFs (for CF/CB = 2:1) reflecting the distributions of solvent molecules with respect to the backbone (B) or the long-alkoxy side chain (C) of the polymer; the results for single-solvent CF system are also shown for comparison. The distance in (b) has been normalized using the mean van der Waals diameters of the two CG particles involved.

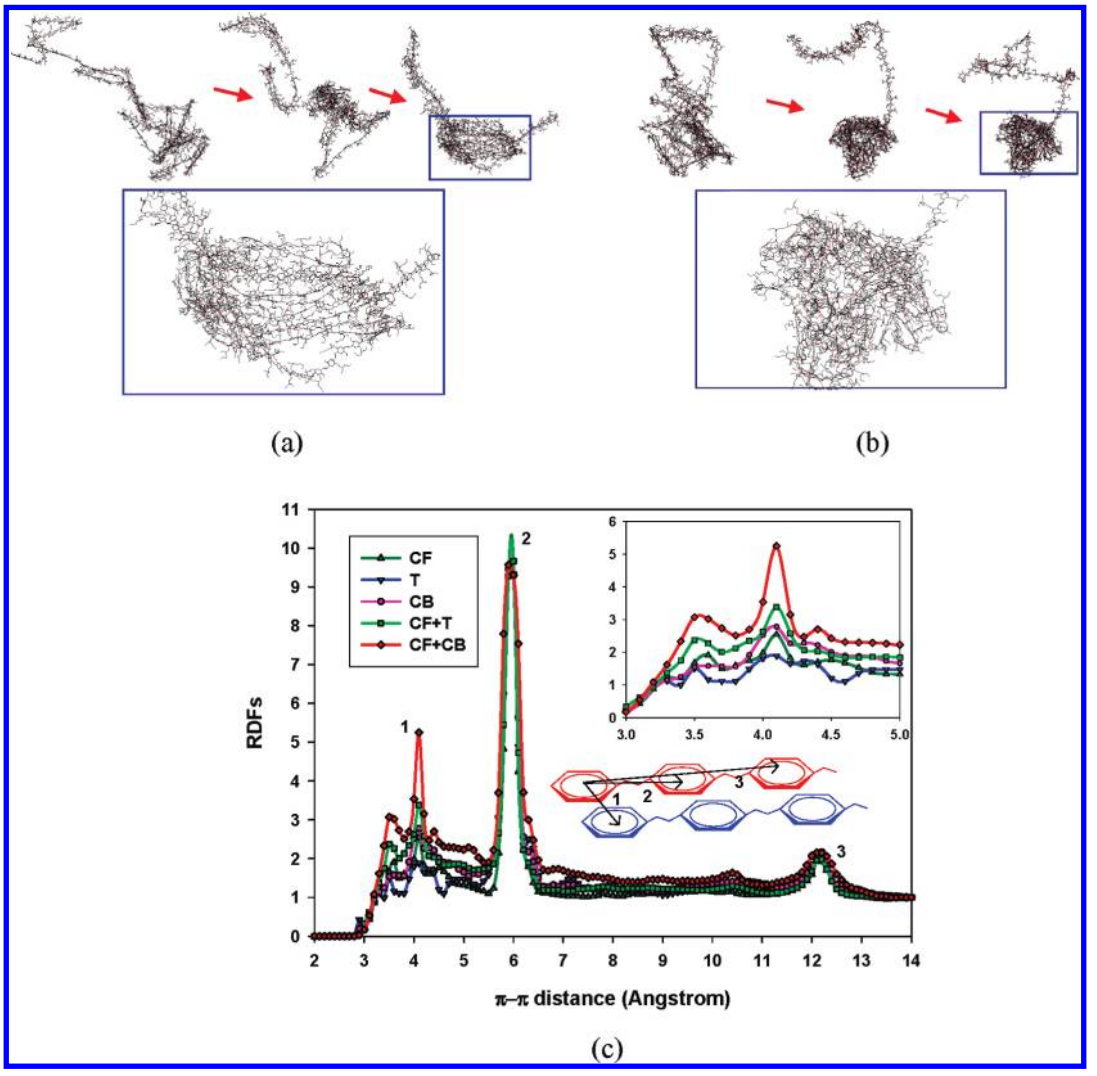

Figure 4. Snapshots of a single 300-mer MEH-PPV chain quenched from (a) a binary-solvent medium, CF/CB = 2:1, and (b) a single-solvent system, T. (c) RDFs revealing the formation of ordered $\pi-\pi$ stacking for a single MEH-PPV chain quenched from various solvent media, where the inset shows the zoomed plot that best illuminates the relative partition of $\pi-\pi$ stacking (at ca. 4.1 Å).

by exploiting hybrid solvents. In the following discussion, we focus on the case with CF/CB binary-solvent system of MEH-PPV; the general observations apply to CF/T system equally well.

Solvent Particle Distributions in Hybrid Solvent Media. To resolve the polymer−solvent interactions, we have examined the detailed solvent particle distributions in the vicinity of the MEH-PPV chain. As schematically shown in Figure 3a, the

distance has been measured in a normally outward direction of each backbone unit. It is significant to notice the ubiquity of a "boundary layer", ca. 2.5 nm in thickness, within which the ratio of the two different solvent particles derails the bulk one considerably. In particular, the (positive) deviation seems to be most prominent at a mixing ratio of CF/CB = 2:1, for which the mean coil size in Figure 2 was also suggestive of an optimal solvent quality. Similar features have been noted for the binary-solvent system with CF/T = 1:1. On the other hand, the first (and dominant) peak appearing in the RDF of Figure 3b clearly indicates that while CF molecules are considerably more attractive to the alkoxy side-chain units (C) of MEH-PPV, CB molecules are slightly more attractive to the backbone (B). An intriguing feature is that both curves (i.e., C−CF and B−CB) display conspicuous oscillations beyond the first peak, a phenomenon rarely observed with single-solvent systems. The sketch given in the same figure suggests this peculiar feature could be indicative of a somewhat ordered, lattice-like structure of solvent molecules encompassing the polymer units that are attractive to them. Another significant finding is that, as one compared the RDFs with the ones for single-solvent (pure) CF system, there is evidently a much greater partition of CF molecules enclosing the MEH-PPV chain in the CF/CB = 2:1 binary solvent medium. That is, without the presence of CB molecules, CF is normally depleted from the polymer territory, possibly to avoid the backbone molecules.

Overall, we suggest the following physical picture to accommodate the anomalous features noted above, which have intriguing consequences as we discuss momentarily on the quenched-chain morphologies. The role played by CB molecules in the CF/CB hybrid solvent system of MEH-PPV is twofold: They attract, and thus "stabilize", the MEH-PPV backbone, preventing too collapsed a chain conformation, especially with the presence of the "disliked" CF molecules that are to be avoided by the phenyl backbone. On the other hand, they help shield the "repulsions" directly between CF and MEH-PPV backbone, thus encouraging immigration of CF molecules into the "boundary layer" regime to attract the side-chain groups more effectively. Altogether, this sophisticatedly compromised, local molecular environment warrants the sustainability of exceptional, highly extended MEH-PPV chains—*which obviously require a free exposure of both the side-chain and backbone units that can only be fulfilled in a hybrid-solvent medium for an amphiphilic polymer like MEH-PPV*. Further, compared with toluene (T) molecules, the somewhat amphiphilic attribute of CB is expected to be a superior "mediator" to play the essential roles as suggested above, besides its better affinity to the CF molecule as well. Note, however, that as CF molecules progressively migrate into the boundary layer regime, they must do so against the bulk osmotic pressure, until an eventual balance between the two "phases" has been established. Thus, the peculiar features manifested by Figures 2 and 3 may be perceived as arising from a subtle balance between local-phase chemical affinities and bulk-phase osmotic pressure—the latter being basically entropic in nature.

Quenched-Chain Nanomorphology and $\pi-\pi$ Stacking. The other primary goal of this simulation is to uncover the exact pathway through which solvent-induced chain conformation might dictate the quenched-chain morphologies upon solvent evacuation. Thus, we performed a systematic backmapping to return the CG model system to full-atom representations in a way as detailed before,[11,35] so as to account for the effects of localized, anisotropic $\pi-\pi$ interactions that cannot be captured in the CG polymer model, although this specific interaction force plays only minor roles in affecting fundamental chain structures in solution, where thermal agitations of the solvent molecules significantly impede the efficacy of highly anisotropic interactions in dilute, semiflexible polymer solution.[11] In Figure 4a,b, two representative cases are examined, revealing the detailed mechanisms of chain quenching as subject to their prior solvent-induced chain conformations. Note that the quenching process simulated here, with an instant solvent evacuation, represents a considerably simplified scenario that is aimed to capture the most elementary molecular features independent of the details of a real film casting. The simulation of chain quenching was carried out in a vacuum, *NVT* environment at the same system temperature (i.e., 298 K), and the time required for a complete chain collapsing is estimated to be ca. 2.0 ns based on the time-dependent mean radius of gyration of the quenched chain. In fact, such an extremely short period compared with the time scales associated with typical film casting might, at least in part, be utilized to justify omitting the effects of solvent evaporation rate.

It is evident that a previously extended and loose chain conformation, such as that formed in the CF/CB = 2:1 medium, permits a relatively regular chain folding along the pivotal tetrahedral defects and, in turn, results in a notably higher degree of ordered $\pi-\pi$ stacking, which promotes the electronic delocalization quintessential for local charge transports. Note, in particular, that the eventual quenching structure shown in Figure 4a has been arrested by localized, anisotropic $\pi-\pi$ interactions. In contrast, for a previously compact chain conformation, such as that formed in toluene and shown in Figure 4b, the quenched chain ubiquitously becomes much collapsed and featureless due to the predominant, isotropic van der Waals segmental interactions. Quantitatively, Figure 4c (which has been created using time plus ensemble averaging as noted earlier) shows the RDFs revealing the fingerprint of ordered $\pi-\pi$ stacking, which bears a characteristic center-to-center distance about 4.1 Å—or about 3.5 Å for the vertical distance between the two phenyl planes, as is more often referred to—for MEH-PPV chains quenched from various solvent media. Clearly, the chain quenched from the CF/CB = 2:1 solvent medium accommodates the greatest amount of $\pi-\pi$ stacking, about 60% higher than the second place for CF/T = 1:1 medium and substantially surpassing the rest single-solvent systems. Moreover, a close correspondence between the mean coil size (or effective solvent quality) in solution, as revealed in Figure 2, and the degree of $\pi-\pi$ stacking in the quenching state can be observed. An interesting exception should be noted, however, with the case of single-solvent CB medium, which apparently results in a higher degree of $\pi-\pi$ stacking despite a smaller mean coil size than in the single-solvent CF medium. The disparity may be explicated by noting that the CB-induced backbone exposure—as contrasted with the CF-induced side-chain exposure—of MEH-PPV evidently serves as an advantageous precursor for the subsequent $\pi-\pi$ stacking. Thus, not only does the overall chain expansion in solution matter, the detailed solvent-induced chain conformation has an important impact on quenched-chain morphologies as well.

To this end, some recent experimental trends are worth noting. Although most experiments conducted involving the use of hybrid solvents for conjugated polymers including MEH-PPV displayed the more regular features as might be foreseen on the basis of simple mixing rules, there were a few occasions when observations evidently defy this commonplace trend. First, we mention that the systematic measurements recently conducted by Chen's group[10] have clearly indicated that the film and device performances of

MEH-PPV can be substantially improved by mixing CF with CB at a volume ratio of CF/CB = 3:1, which is close to a number ratio of CF/CB = 2:1 as simulated here. They have attributed the general improvement to the formation of spatially homogeneous distribution of ordered structures (well-packed chains and/or aggregates), with yet unknown mechanisms. For solution samples, the photoluminescence features (Figure 2 in ref 9) reported by Zhang and co-workers for MEH-PPV in the hybrid solvent medium chloroform/cyclohexane inhabited a clearly nonsystematic trend with varying compositions, resembling the phenomenon seen in Figure 2. No similar features were noted, however, for the other solution system made of chloroform and methanol, two solvents that are more alike.

Conclusions

This multiscale simulation of a standard amphiphilic conjugated polymer has unraveled an unequivocal pathway via which specific solvents or hybrid solvents may be exploited to control ordered nanostructures—the $\pi-\pi$ stacking—in the quenching state. The sophisticatedly compromised, local-phase molecular environment as has been disclosed for two representative binary (aliphatic/aromatic) solvent media of MEH-PPV not only renders in-depth insight into fine morphological controls in amphiphilic polymer solution but also points to the open opportunity of propelling the frontier performances of conjugated polymer thin films when cast from optimum hybrid solvent media.

Acknowledgment. The authors thank the reviewers for useful comments/suggestions. This work is supported by the National Science Council of ROC under Grant NSC99-2120-M007-012. Resources provided by the National Center for High-Performance Computing are also acknowledged.

Supporting Information Available: Detailed system descriptions, comparisons between the CG and AMD simulations on the predicted bond length/angle distributions (Figure S1), RDFs of individual particle baths (Figure S2), and RDFs of polymer−solvent pairs in CF/CB = 2:1 medium (Figure S3) as well as all potential functions and parameters (Table S1). This material is available free of charge via the Internet at http://pubs.acs.org.

References and Notes

(1) Burroughes, J. H.; Bradley, D. D. C.; Brown, A. R.; Marks, R. N.; Mackay, K.; Friend, R. H.; Burn, P. L.; Holmes, A. B. *Nature* **1990**, *347*, 539.
(2) Braun, D.; Heeger, A. J. *Appl. Phys. Lett.* **1991**, *58*, 1982.
(3) Friend, R. H.; Gymer, R. W.; Holmes, A. B.; Burroughes, J. H.; Mark, R. N.; Taliani, C.; Bradley, D. D. C.; Dos Santos, D. A.; Brlédas, J. L.; Löglund, M.; Salaneck, W. R. *Nature* **1999**, *397*, 121.
(4) Yu, G.; Gao, J.; Hummelen, J. C.; Wudl, F.; Heeger, A. J. *Science* **1995**, *270*, 1789.
(5) Günes, S.; Neugebauer, H.; Sariciftci, N. S. *Chem. Rev.* **2007**, *107*, 1324.
(6) Dennler, G.; Scharber, M. C.; Brabec, C. J. *Adv. Mater.* **2009**, *21*, 1323.
(7) Nguyen, T. Q.; Doan, V.; Schwartz, B. J. *J. Chem. Phys.* **1999**, *110*, 4068.
(8) Shi, Y.; Liu, J.; Yang, Y. *J. Appl. Phys.* **2000**, *87*, 4254.
(9) Zhang, H.; Lu, X.; Li, Y.; Ai, X.; Zhang, X.; Yang, G. *J. Photochem. Photobiol. A* **2002**, *116*, 143.
(10) Chen, M. C.; Hung, W. C.; Su, A. C.; Chen, S. H.; Chen, S. A. *J. Phys. Chem. B* **2009**, *113*, 11124.
(11) Lee, C. K.; Hua, C. C.; Chen, S. A. *J. Phys. Chem. B* **2009**, *113*, 15937.
(12) Tschöp, W.; Kremer, K.; Batoulis, J.; Bürger, T.; Hahn, O. *Acta Polym.* **1998**, *49*, 61.
(13) Reith, D.; Meyer, H.; Müller-Plathe, F. *Macromolecules* **2001**, *34*, 2335.
(14) Shelley, J. C.; Shelley, M. Y.; Reeder, R. C.; Bandyopadhyay, S.; Klein, M. L. *J. Phys. Chem. B* **2001**, *105*, 4464.
(15) Fukunaga, H.; Takimoto, J. I.; Doi, M. *J. Chem. Phys.* **2002**, *116*, 8183.
(16) Faller, R.; Reith, D. *Macromolecules* **2003**, *36*, 5406.
(17) Reith, D.; Pütz, M.; Müller-Plathe, F. *J. Comput. Chem.* **2003**, *24*, 1624.
(18) Clancy, T. C. *Polymer* **2004**, *45*, 7001.
(19) Faller, R. *Polymer* **2004**, *45*, 3869.
(20) Marrink, S. J.; de Vries, A. H.; Mark, A. E. *J. Phys. Chem. B* **2004**, *108*, 750.
(21) Boek, E. S.; Padding, J. T.; den Otter, W. K.; Briels, W. J. *J. Phys. Chem. B* **2005**, *109*, 19851.
(22) Li, X.; Ma, X.; Huang, L.; Liang, H. *Polymer* **2005**, *46*, 6507.
(23) Harmandaris, V. A.; Adhikari, N. P.; van der Vegt, N. F. A.; Kremer, K. *Macromolecules* **2006**, *39*, 6708.
(24) Li, X.; Kou, D.; Rao, S.; Liang, H. *J. Chem. Phys.* **2006**, *124*, 204909.
(25) Shih, A. Y.; Arkhipov, A.; Freddolino, P. L.; Schulten, K. *J. Phys. Chem. B* **2006**, *110*, 3674.
(26) Carbone, P.; Negri, F.; Müller-Plathe, F. *Macromolecules* **2007**, *40*, 7044.
(27) Santangelo, G.; Matteo, A. D.; Müller-Plathe, F.; Milano, G. *J. Phys. Chem. B* **2007**, *111*, 2765.
(28) Spyriouni, T.; Tzoumanekas, C.; Theodorou, D.; Müller-Plathe, F.; Milano, G. *Macromolecules* **2007**, *40*, 3876.
(29) Carbone, P.; Varzaneh, H. A. K.; Chen, X.; Müller-Plathe, F. *J. Chem. Phys.* **2008**, *128*, 064904.
(30) Karimi-Varzaneh, H. A.; Carbone, P.; Müller-Plathe, F. *J. Chem. Phys.* **2008**, *129*, 154904.
(31) Lee, C. K.; Hua, C. C.; Chen, S. A. *J. Phys. Chem. B* **2008**, *112*, 11479.
(32) Noid, W. G.; Chu, J. W.; Ayton, G. S.; Krishna, V.; Izvekov, S.; Voth, G. A.; Das, A.; Andersen, H. C. *J. Chem. Phys.* **2008**, *128*, 244114.
(33) Noid, W. G.; Liu, P.; Wang, Y.; Chu, J. W.; Ayton, G. S.; Izvekov, S.; Andersen, H. C.; Voth, G. A. *J. Chem. Phys.* **2008**, *128*, 244115.
(34) Peter, C.; Site, L. D.; Kremer, K. *Soft Matter* **2008**, *4*, 859.
(35) Lee, C. K.; Hua, C. C.; Chen, S. A. *J. Chem. Phys.* **2010**, *133*, 064902.
(36) Hu, D.; Yu, J.; Wong, K.; Bagchi, B.; Rossky, P. J.; Barbara, P. F. *Nature* **2000**, *405*, 1030.
(37) Sumpter, B. G.; Kumar, P.; Mehta, A.; Barnes, M. D.; Shelton, W. A.; Harrison, R. J. *J. Phys. Chem. B* **2005**, *109*, 7671.
(38) Inigo, A. R.; Chiu, H. C.; Fann, W.; Huang, Y. S.; Jeng, U. S.; Hsu, C. H.; Peng, K. Y.; Chen, S. A. *Synth. Met.* **2003**, *139*, 581.